

Subsurface Imaging of Dielectric Objects Buried under Rough Surface

Esin Karpat

Abstract— In this paper, a distance measurement based reflection point terrain estimation method (RPTEM) for characterizing two-dimensional (2-D) rough surfaces is presented. The method is based on the analysis of time-domain field data obtained by GPR system with Synthetic Aperture Radar (SAR) scan over 2-D rough ground surfaces. The distance from each antenna position to the ground surface is established from the late time responses of each antenna. The distance information extracted from the reflected signal is used to create an estimate of the rough ground. A circle is considered with a corresponding radius, which is the distance information, with the antenna location at its center. An outline of the terrain is obtained through the overlapping circles at neighboring antennas. The terrain profiles obtained via both SAR-processing and the RPTEM are discussed and compared with the actual geometry. The results show good agreement between the imagery of the surface height distribution obtained by RPTEM, SAR processing and the actual geometry of the 2-D rough surfaces. Time consumed for image reconstruction is discussed for each method.

Keywords— Electromagnetic scattering, signal processing, image processing, ground penetrating radar (GPR), surface reconstruction; FDTD.

I. INTRODUCTION

GROUND surfaces are not flat but rough in real life. In subsurface imaging, surface reconstruction is an important feature. In order to be able to detect the small dielectric objects (such as nonmetallic anti-personnel mines) located beneath the 2-D rough ground surfaces or tumors under human body, the profile of rough surfaces must be obtained so that the effect of surfaces can be digitally eliminated from the measured data. So the reconstruction of the real 2-D surface is very challenging for several imaging problems.

The dominant reflection in the scattered field in subsurface imaging is due to the ground surface. This reflection contains information such as the distance of the ground from the antenna location and the electrical properties of the ground. The distance information extracted from the reflected signal can be used to obtain the outline of the rough surface.

Radar-based microwave imaging techniques typically require the antennas to be placed at a certain distance from or on the surface. This requires prior knowledge of the surface location, shape, and size. There are several methods such as peak detection, impulse response methods in the literature [1-

7]. In tissue sensing adaptive radar (TSAR) algorithm, the outline of the breast and the thickness of the breast skin [6] is obtained by analysing the reflected signal. A deconvolution technique is applied to find the impulse response with respect to a known reflected signal. Impulse response method is used to estimate the surface location.

There are a variety of image and signal processing methods proposed [8, 9]. El-Shenawee et.al used SDFMM method to reconstruct the terrain profile of the rough ground surface [8], which was originally developed by Jandhyala, Michielssen, and Chew ([10-12]) to analyze 3-D scattering problems of quasi-planar structures.

In RPTEM, the function of the terrain profile is obtained approximately, which can be used for further processing approaches. However, in SAR processing, used in this paper, we just obtain the image of the terrain and have no digital information about the terrain profile. In addition, RPTEM is faster when compared with the other one.

In this paper, the methods used to reconstruct surface image are discussed in the following section and the results obtained via both method are given in the third section. In the fourth and fifth sections, the conclusion of the paper and the progressive studies are explained in the following sections.

II. METHODS

A recently introduced GrGPR, virtual tool is used to generate synthetic data for sample scenarios [13-15]. In the simulations 50 transmitter/receiver antennas are placed over terrain and activated sequentially as in SAR principle or we can assume that a transmitter/receiver antenna pair is activated in 50 different positions over terrain (Fig. 1). The GrGPR receiver records time-domain raw signals, which contains both early- and late-time responses, for each antenna position. Early-time response consists of the transmit signal and the signal reflected from the boundary/ skin layer. The transmit signal received directly by the receiver is orders of magnitude higher than the signal backscattered from the surface under investigation. The reflected signals are analyzed and focused to create images that indicate the location of strongly scattering objects/ground surface. Then as described in the following subsections the received raw signals are processed in order to obtain surface profiles.

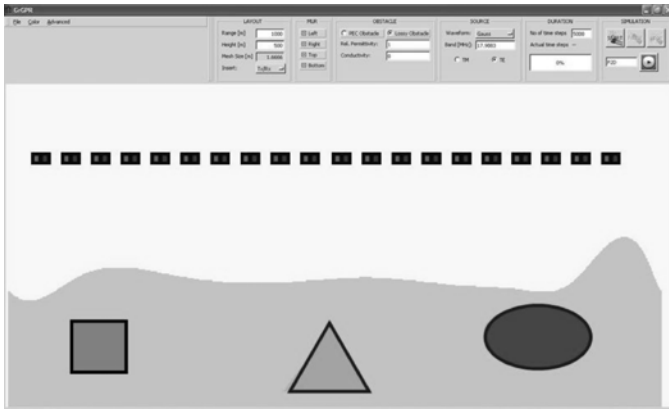


Fig. 1 GrGPR simulator , and a sample scenario with a number of radiator/receiver pairs located over the surface.

A. SAR Processing

Early time response, which is orders of magnitude higher than the signal backscattered from the surface under investigation, must be removed prior to the application of SAR procedure. Different techniques may be used for this purpose; performing the simulations twice; with and without the object under investigation, and then subtracting one from the other. In this study, GrGPR simulations are repeated for free space and early-time response is removed accordingly.

The accumulation of late-time responses from every single cell to a pair of radiator/receiver necessitates the calculation of round-trip signal delay. Denote coordinates of each cell/pixel by (x_i, y_j) where x and y are the horizontal and vertical axes, respectively. Coordinates of the k^{th} radiator/receiver pair is denoted by (x_{tr}^k, y_{tr}^k) . The time necessary for a round-trip from the radiator to the cell/pixel, and back to the receiver can then be calculated via

$$\tau_{i,j}^k = \frac{2 * \sqrt{(x_i - x_{tr}^k)^2 + (y_j - y_{tr}^k)^2}}{c} \tag{1}$$

Where, c is the speed of light. The corresponding pixel (distance) index $l_{i,j}^k$ is directly obtained from

$$l_{i,j}^k = \frac{\tau_{i,j}^k}{\Delta t} \tag{2}$$

Where Δt is the FDTD time step. The field intensity of each cell (i.e., the image color) is then formed as

$$I(i, j) = \sum_{k=1}^N a_{i,j}^k (l_{i,j}^k) \tag{3}$$

Where $a_{i,j}^k$ is the intensity at calculated distance $l_{i,j}^k$. In summary, the three step SAR algorithm is based on, early-time response elimination and signal enhancement, the calculation of the time delays of all roundtrips from all pixels to all scan points and superposing scattered field values corresponding to those delays.

B. Reflection Point Terrain Estimation Method (RPTEM)

Reflection point estimation method (RPTEM), is based on identifying the time step that the reflection from the surface had occurred. In this method, different than SAR processing, the GrGPR is run only once and the reflected fields are stored for each antenna position. As an inverse problem, the time domain reflected fields are then analyzed to obtain the corresponding pixel (distance) index at which reflection from the surface had occurred.

The reflected signal is digitized according to a threshold value. The absolute values which are greater than the threshold are assumed to be “1” and the rest is “0” (4).

$$F(n) = \begin{cases} 1, & \text{abs}(f(t)) \geq T_r \\ 0, & \text{abs}(f(t)) < T_r \end{cases} \tag{4}$$

where T_r is a *Threshold* value very close to “0”. Then the time steps where these level transitions and therefore the reflections accrued are obtained (Fig. 2a). An enlarged form of the figure is also given in Figure 2b.

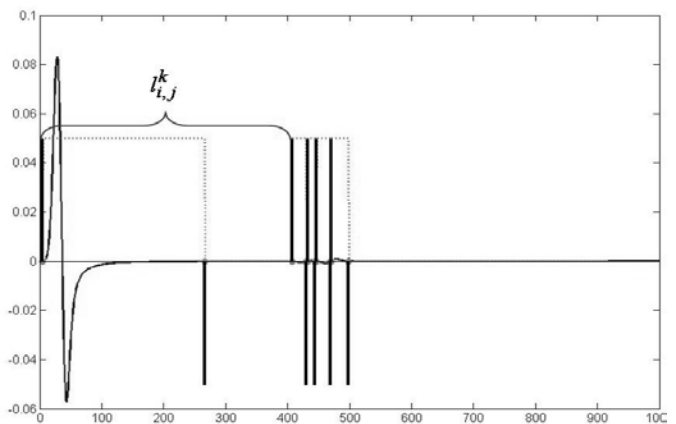


Fig. 2a. The analyzed reflected signal with early- and late-responses

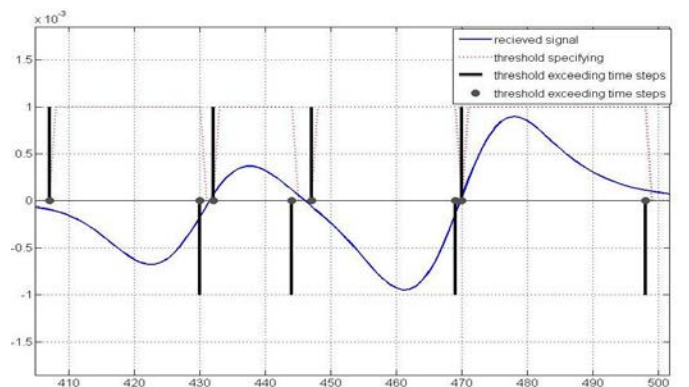


Fig. 2b. The enlarged image of the analyzed signal

The round-trip time delay is calculated via Eq.5.

$$\tau_{i,j}^k = l_{i,j}^k * \Delta t \tag{5}$$

As the time step when the reflection from ground occurred is obtained, the probable indices that the reflection could possibly come about are calculated. A circle may be considered with a corresponding radius of r^k with the antenna location (x_{ir}^k, y_{ir}^k) at its center (6). The overlapping circles at neighboring antennas create an outline of the terrain estimate [2].

$$r_i = \frac{\tau_{i,j}^k * c}{2}$$

$$x_c^{(n)} = x_c^{(n-1)} - r_i * \cos \theta$$

$$y_c^{(n)} = y_c^{(n-1)} + r_i * \sin \theta$$
(6)

where (x_c, y_c) represent the pixels on that circle. This approach is consistent with currently used omnidirectional antenna.

Intersecting or neighboring pixels are found on these circles for each consecutive antenna locations where the reflection assumed to occur on the surface of the terrain. Then the cubic-spline algorithm is applied to interpolate and find out the best curve function to fit the reflection points obtained on the terrain profile. A hybrid subsurface imaging and ray tracing algorithm developed for subsurface imaging analysis.

C. A Hybrid Subsurface Imaging-Ray Tracing Algorithm

Each antenna is activated sequentially. The propagation space is assumed to be divided into sub-layers with a refraction index of n . The rays emitted from antennas are propagated in space until they reach the reconstructed terrain profile. The direction of the rays are calculated according to snell's law (7). The ray paths are given in Fig. 3.

$$n_i \sin \theta_i^k = n_t \sin \theta_t^k$$
(7)

The distance from antenna to the corresponding pixel and therefore the time delay is calculated for each ray via Eq. (2). Superposition of scattered field gives the position of the scatterer as in SAR processing (3).

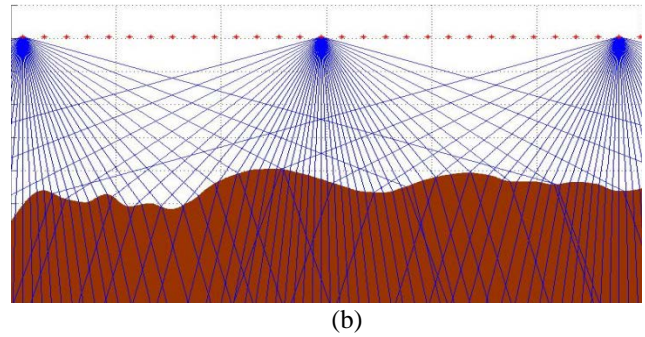
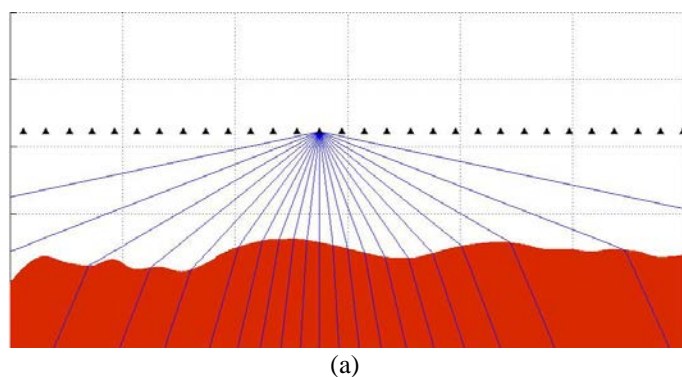


Fig 3 Ray paths propagating through rough surface

III. RESULTS

Terrain profiles obtained by proposed method RPTEM are compared with the images obtained via SAR processing. The results show good agreement with each other. In the following examples, antenna pairs are located 150 cells above the rough surface and activated consecutively as in SAR type antenna array. The scattered data received from the ground surface is stored for post-processing in order to obtain terrain profile.

In Figure 4a and b, the terrain profile is obtained with both SAR processing and RPTEM, respectively. The obtained profiles are compared with the original terrain. The results show that the terrain obtained with RPTEM is in good agreement with the original one.

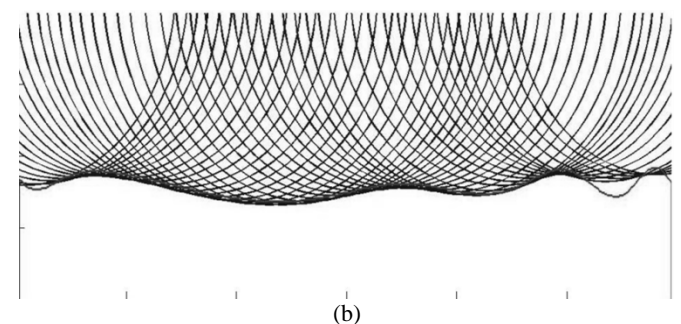
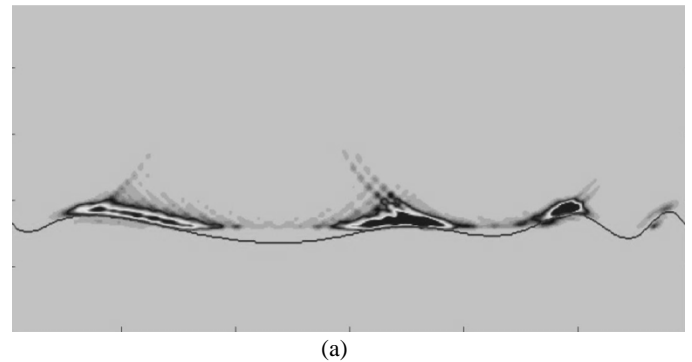


Fig 4 2D images of terrain profile obtained via (a) SAR processing and (b) RPTEM and their comparison with the original GRGPR scenario (solid line)

IV. CONCLUSION

Surface imaging and reconstruction in 2D idealized environments and reconstruction algorithms SAR processing and RPTEM are discussed. A FDTD-based GrGPR virtual tool is used to generate forward scattered data synthetically. The simulations are run for concave/convex and triangle type terrain scenarios. Terrain profiles, obtained with both SAR and RPTEM, are in good agreement with the original one. The calculation time for each method are compared. The results show that RPTEM is much more faster when compared with SAR processing.

REFERENCES

[1] Trevor C. Williams, Elise C. Fear, and D.W. Westwick, "Tissue sensing adaptive radar for breast cancer detection: investigations of reflection from the skin", IEEE Antennas and Propagation Society International Symposium, 2004, pp.2436-2439 Vol.3, 20-25 June 2004.

[2] Trevor C. Williams, Jeff M. Sill, and Elise C. Fear, "Breast Surface Estimation for Radar-Based Breast Imaging Systems", IEEE Transactions On Biomedical Engineering, Vol. 55, No. 6, pp. 1678-1686, June 2008. <http://dx.doi.org/10.1109/TBME.2008.919883>

[3] Trevor C. Williams, Jeff M. Sill, Elise C. Fear, "Robust Approach to Skin Location Estimation for Radar-Based Breast Imaging Systems", 30th Annual International IEEE EMBS Conference, Vancouver, British Columbia, Canada, August 20-24, 2008.

[4] T. C. Williams, E.C. Fear, David T. Westwick, "Tissue sensing adaptive radar for breast cancer detection: investigations of an improved skin sensing method", IEEE Trans. Microwave Theory and Tech., Vol. 54, pp 1308-1314, June 2006. <http://dx.doi.org/10.1109/TMTT.2006.871224>

[5] T. C. Williams, E.C. Fear, "Tissue sensing adaptive radar for breast cancer detection:using a deconvolution method for enhanced skin sensing", IEEE Antennas Propagat. Symposium, Washington, DC, USA, July 2005.

[6] D. W. Winters, J. D. Shea, E. L. Madsen, G. R. Frank, B. D. Van Veen, and S. C. Hagness, "Estimating the breast surface using UWB microwave monostatic backscatter measurements", IEEE Trans. Biomed. Eng., vol. 55, no. 1, pp. 247-256, Jan. 2008. <http://dx.doi.org/10.1109/TBME.2007.901028>

[7] T. C. Williams and E. C. Fear, "Tissue sensing adaptive radar for breast cancer detection: Skin outline creation on a complex simulated hemispherical breast model," IEEE Antennas Propag. Symp., Waikiki, HI, pp. 2156-2159, Jun. 2007.

[8] Magda El-Shenawee, Carey Rappaport, IEEE, Eric L. Miller, and Michael B. Silevitch, "Three-dimensional subsurface analysis of electromagnetic scattering from penetrable PEC objects buried under rough surfaces: Use of the steepest descent fast multipole method (SDFMM)", IEEE Transactions On Geoscience And Remote Sensing, Vol. 39, No. 6, pp:1174-1182, June 2001. <http://dx.doi.org/10.1109/36.927436>

[9] Magda El-Shenawee and Eric Miller, "Inverse Scattering Computational Algorithm for the Reconstruction of Random Rough Surface Profiles" IEEE Antennas and Propagation Society International Symposium, Monterey, California, USA, 20-25 June 2004.

[10] V. Jandhyala, "Fast multilevel algorithms for the efficient electromagnetic analysis of quasi-planar structures," Ph.D. dissertation, Dept. Elect. Comput. Eng., Univ. Illinois, Urbana, 1998.

[11] V. Jandhyala, E. Michielssen, B. Shanker, and W. C. Chew, "A combined steepest descent-fast multipole algorithm for the fast analysis of threedimensional scattering by rough surfaces," IEEE Trans. Geosci. Remote Sensing, vol. 36, pp. 738-748, May 1998. <http://dx.doi.org/10.1109/36.673667>

[12] V. Jandhyala, B. Shanker, E. Michielssen, and W. C. Chew, "A fast algorithm for the analysis of scattering by dielectric rough surfaces," J. Opt. Soc. Amer. A, Opt. Image Sci., vol. 15, pp. 1877-1885, July 1998.

<http://dx.doi.org/10.1364/JOSAA.15.001877>

[13] E.Karpat, M. Çakır, L. Sevgi, "Subsurface Imaging, FDTD-Based Simulations and Alternative Scan/Processing Approaches", Microwave and Optical Technology Letters, vol. 51, no 4, pp. 1070-1075, Apr 2009. <http://dx.doi.org/10.1002/mop.24253>

[14] E. Karpat, "CLEAN Technique to classify and detect targets in subsurface imaging", International Journal of Antennas and Propagation, (in press, 2012), doi: 10.1155/2012/917248. <http://dx.doi.org/10.1155/2012/917248>

[15] E. Karpat, "Subsurface imaging analysis for multiple dielectric objects buried under homogenous ground", International Journal of Advances in Engineering and Technology, IJAET, vol.6, no:1, pp: 12-20, March 2013.